Lab on a Chip

PAPER

View Article Online
View Journal | View Issue

Published on 05 December 2016. Downloaded by Concordia University, Montreal on 19/01/2018 16:00:41.

Cite this: *Lab Chip*, 2017, **17**, 323

On-chip integration of droplet microfluidics and nanostructure-initiator mass spectrometry for enzyme screening†

Joshua Heinemann,[ab] Kai Deng,[ac] Steve C. C. Shih,[f] Jian Gao,[b] Paul D. Adams,[abe] Anup K. Singh[ac] and Trent R. Northen*[abd]

Received 20th September 2016,
Accepted 2nd December 2016

DOI: 10.1039/c6lc01182a

www.rsc.org/loc

Biological assays often require expensive reagents and tedious manipulations. These shortcomings can be overcome using digitally operated microfluidic devices that require reduced sample volumes to automate assays. One particular challenge is integrating bioassays with mass spectrometry based analysis. Towards this goal we have developed μNIMS, a highly sensitive and high throughput technique that integrates droplet microfluidics with nanostructure-initiator mass spectrometry (NIMS). Enzyme reactions are carried out in droplets that can be arrayed on discrete NIMS elements at defined time intervals for subsequent mass spectrometry analysis, enabling time resolved enzyme activity assay. We apply the μNIMS platform for kinetic characterization of a glycoside hydrolase enzyme (CelE-CMB3A), a chimeric enzyme capable of deconstructing plant hemicellulose into monosaccharides for subsequent conversion to biofuel. This study reveals NIMS nanostructures can be fabricated into arrays for microfluidic droplet deposition, NIMS is compatible with droplet and digital microfluidics, and can be used on-chip to assay glycoside hydrolase enzyme *in vitro*.

Introduction

Enzymes are frequently engineered to modify their function or catalytic efficiency[1–3] to increase product yields significantly through the use of directed evolution or rational protein design.[4,5] Mass spectrometry is a label-free detection technique for measuring biochemical activity and has for some become the method of choice for high throughput assays.[6,7] Unfortunately, the traditional mass spectrometry approaches for screening samples are slow and require large sample volumes often making them cost prohibitive for high throughput screening efforts.[8,9]

Nanostructure-initiator mass spectrometry (NIMS) is a laser desorption/ionization approach that offers very high throughput and requires very small amounts of samples. It directly measures the substrates and products of enzymatic reactions and is broadly applicable to many molecule classes including metabolites, drugs and peptides,[6,10–12] and has been developed to rapidly analyse enzyme activities to support the development of improved biomass degrading enzymes.[13] NIMS uses liquid (initiator) coated silicon nanostructures to generate gas phase ions from surface adsorbed molecules upon laser irradiation. Hence it lends itself to microfabrication allowing biochemical reactions as low as 1 nl of deposited sample. The use of acoustic printing with NIMS has shown much promise for large-scale screening efforts, *in vitro* expression and analysis of enzyme activities.[6,13,14] One limitation of this approach, is the dead-volume required to print from 384-well plates is approximately 20 μl making it expensive to perform large-scale screening. Since NIMS is fabricated from silicon based material, it is well suited for integration with microfluidics, offering the potential to conduct assays in picoliter droplets which greatly reduces cost and increases throughput potential.[15–17]

There are numerous examples of integrated microfluidic/mass spectrometry, from electrospray ionization (ESI) to matrix assisted laser desorption ionization (MALDI).[18,19] Two such approaches show integration of MALDI with microfluidics is useful for both peptide,[20] and protein identification.[21] Programmable control of digital microfluidic functions enables droplet operations, which are likely improvements for enzymatic functional screening, because of electronic timing and control.[22–24] Typical NIMS assays

[a] *Joint Bioenergy Institute, Emeryville, California 94608, USA*
[b] *Lawrence Berkeley National Laboratory, Berkeley, California 94720, USA. E-mail: trnorthen@lbl.gov*
[c] *Sandia National Laboratories, Livermore, California 94551, USA*
[d] *Joint Genome Institute, Walnut creek, California, 94598, USA*
[e] *Department of Bioengineering, University of California, Berkeley, California, 94720, USA*
[f] *Department of Electrical and Computer Engineering, Concordia University, Montreal, Quebec, Canada*

† Electronic supplementary information (ESI) available. See DOI: 10.1039/c6lc01182a

Published on 05 December 2016. Downloaded by Concordia University, Montreal on 19/01/2018 16:00:41.

require a washing step to remove cell debris which often interferes with mass spectrometry analysis,[15,25] using microfluidics could allow automated sample processing using electro-wetting on dielectric (EWOD), to automate this process.[26,27] In addition, integrated digital droplet devices have the potential to effectively array droplets onto the NIMS surface, adsorbing the substrates and products, and then removing the droplet to minimize ion suppression from salts *etc.*[28–30] Recent applications show combined droplet and digital microfluidics is suitable for programming diverse biochemical operations including genomic assembly, transformation and culture.[27,31]

Here we integrate microfluidics with NIMS in a platform we refer to as μNIMS. μNIMS enables digital control of

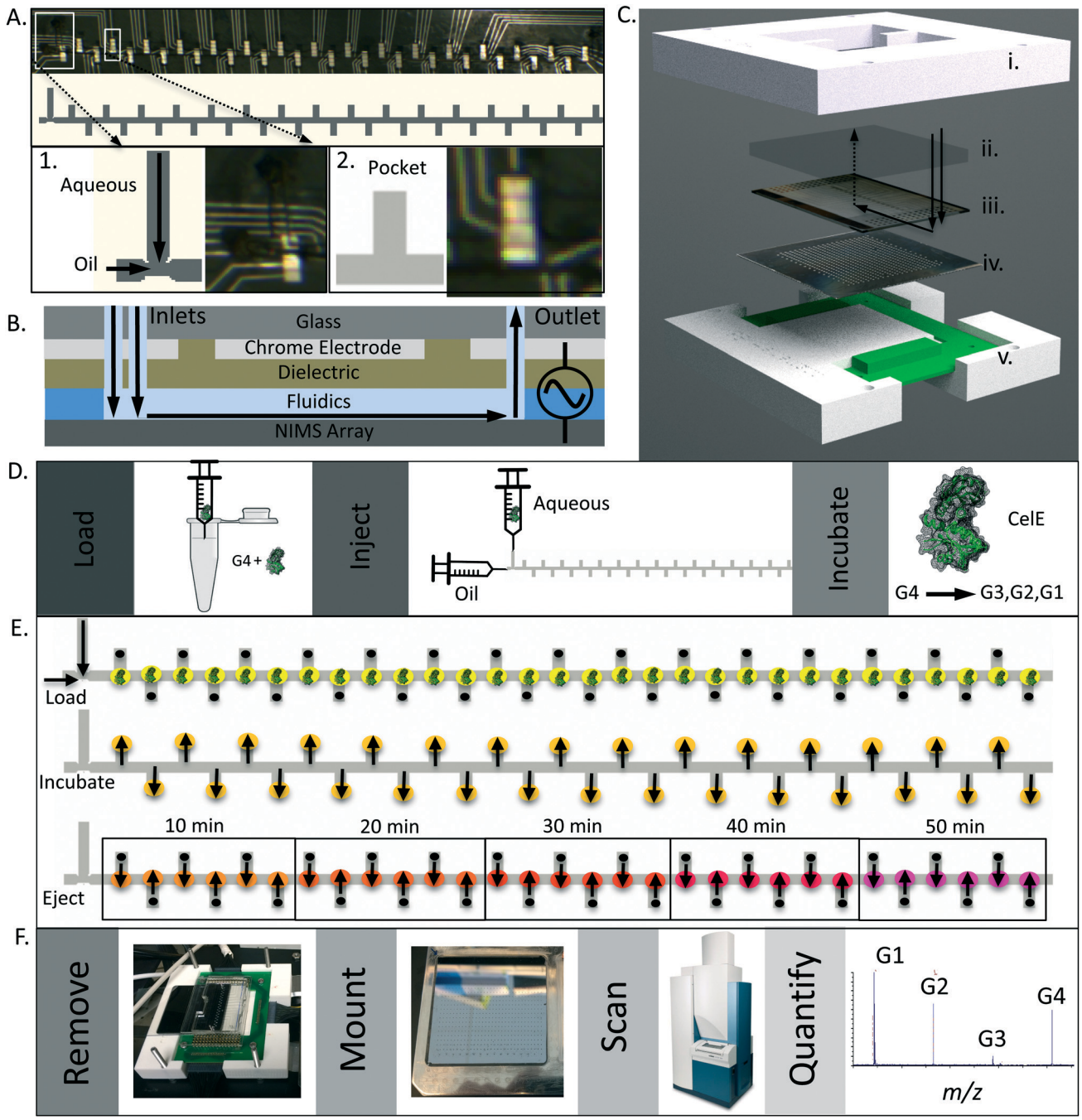

Fig. 1 μNIMS assembly and operation. A. Electrode and fluidics design, layer iii. Inset: 1. t-junction, arrows show direction of flow, 2. μNIMS pocket, B. Digital microfluidics chip, compression sealed to the NIMS array, C. the stack for holding the layers together. i. 3D printed top, ii. PDMS mounting layer for interfacing fluidics to microfluidics, iii. Chip containing the electrodes, dielectric and fluidics, iv. NIMS chip, v. bottom piece with dropbot adapter, D. operation workflow E. Inject: chip is filled with droplets, load: flow is stopped and droplets are loaded onto the NIMS array for incubation and probe deposition, eject: the droplets are incubated for 10, 20, 30, and 40 minutes over six successive pads and then actuated into the central chamber where they are then evacuated, F. workflow of NIMS array removal and analysis.

 This journal is © The Royal Society of Chemistry 2017

Published on 05 December 2016. Downloaded by Concordia University, Montreal on 19/01/2018 16:00:41.

enzymatic time course for cellulose-degrading enzyme using NIMS as a biosensor. The chip moves droplets onto a NIMS surface, incubates and then removes after a defined period of time. Probe sorbs to the NIMS surface allowing mass spectral kinetic characterization of cellulose degrading enzymes. This technology is appealing because it has programmable time resolution, scalable density, and can be more broadly applied.

Results

Integrated microfluidics-NIMS device

The major design objective for the μNIMS device was to deposit sample solutions at specified two-dimensional locations on the NIMS array in a time dependent manner. The microfluidics chip consisted of chrome electrodes over a central fluidics channel (Fig. 1). The chip contained two basic functions, a t-junction for droplet generation (Fig. 1A. 1.), and 31 digital arrayers for droplet actuation over NIMS pads (Fig. 1A. 2.). The t-junction used pressure driven flow to break aqueous enzyme/substrate plugs into droplets of approximately 150 nl using immiscible oil phase similar to previous demonstration.[32] The chip contained glass substrate, chrome electrodes, dielectric, and fluidics made the top of the stack for interfacing with the NIMS array, which also functioned as a ground plate during digital actuation (Fig. 1B.). The PDMS fluidics layer sealed reversibly to the NIMS array allowing selective droplet actuation onto each NIMS pad (Fig. 1A.). The final design loaded droplets in parallel, but the droplets could also be loaded serially if desired (Supplementary Video†). The glass layer contained fluidic access ports and is coated with 124 chrome electrodes for directing droplets into pockets (Fig. 1B.). The reversible seal between the fluidics chip and NIMS array allowed removal and placement into the mass spectrometer (MS) for imaging. Arrayers were aligned with NIMS pads (Fig. 1C. iv.), which allowed droplets to be deposited onto the array (Fig. 1C.) The stack holding the layers together was made of a 3D printed chassis (Fig. 1C. i. v.), where the bottom layer also contained pogo pins in printed circuit board for integration with dropbot control hardware.[33] An upper gasket made of PDMS sat between the 3D printed chassis and DMF chip to allow interfacing with PEEK tubing (Fig. 1C. ii.).

Fluidics operation

CellE enzyme cocktail was loaded onto the device by filling syringe tubing with 6 μl plugs of pre-mixed enzyme substrate cocktail and injected onto the chip, where droplets were incubated (Fig. 1D.). Plugs were broken into droplets at the t-junction and spaced using droplet synchronization, which matches droplet formation with the actuation of electrodes to create perfectly spaced droplets (Supplementary Video†). When the central chamber was filled with droplets syringe pumps are stopped while holding a low voltage (20 V) on the electrodes to hold droplets in position outside the pocket (Fig. 1E., load). Droplets of enzyme cocktail were then actuated onto the μNIMS pads where they were incubated for a period of time, this allowed G4 to be converted and sorbed to NIMS pad (Fig. 1E., incubate). At the specified time intervals, droplets were ejected from the pocket (Fig. 1E., eject). The incubation of the droplet over the pads on the NIMS array allowed substrates and products to sorb from the droplet. The digital actuation functioned to move droplets from the central chamber, in and out of the pocket containing the NIMS active pad allowing substrate and product to sorb. This is consistent with the normal operation of NIMS. Droplets are loaded after pausing flow in this experiment, but demonstrations show droplets can also be removed directly from flow if desired (Supplementary Video†). MS imaging of the silicon wafer after exposure to standard revealed that fluorous tagged substrates stay adsorbed onto the NIMS pads in our microfluidic environment when incubating the droplet over a pad, similar to traditional NIMzyme execution.[15]

NIMS array

NIMS pads are fabricated using photopatternable PDMS[34] as a protective gasket over a laser cut silicon wafer (5×5 cm^2) before reactive ion etching (DRIE)[16] very similar to the original design of desorption ionization on silicon surfaces.[35] Exposure etches the silicon wafer to create surface nanostructures (Fig. 2B. and C.), for NIMS analysis. To test the ability to deposit samples onto the NIMS pads and subsequently perform mass spectrometry analysis, the metabolite standard, dextromethorphan was used, where droplets were deposited over pads. Following deposition, the chip was removed and mass spectrometry imaging was performed to map dextromethorphan (m/z 272) across the surface. Subsequent processing using OpenMSI[36] confirmed successful analyte deposition (Fig. 2D.). Droplets of 1,4-*b*-D-cellotetraose-probe (G4) substrate were spotted onto the μNIMS pads during enzymatic reaction for confirmation of applicable use in monitoring cellulose degradation. However, the ion intensities were low compared to the dextromethorphan and it was necessary to perform mass spectrometry imaging to detect all desired degradation products presumably due to suppression from the surfactant used to stabilize the droplets (Fig. 3).

Application to glycoside hydrolase analysis

We tested μNIMS ability to quantify enzyme kinetics using a chimeric enzyme made up of a broad specificity GH hydrolase family 5 (GH5) domain from C. Thermocellum (Cthe_0797) fused onto a carbohydrate binding module, CBM3a (CelE)[37] we applied the μNIMS to compare the reaction kinetics of, CelE, against cellotetraose at two different pHs. Briefly, purified endogluconase, CelE was reacted with 1,4-*b*-D-cellotetraose-probe (G4) substrate-probe G4 in either phosphate buffer (pH = 6) (Fig. 4A.) or 100 mM acetate buffer (pH = 5) (Fig. 4B.) and analysed every 10 min using μNIMS as described above. Reaction solutions were premixed in a 0.5 ml eppendorf tube, by adding buffer, substrate and enzyme and premixing to a final volume of 6 μl. The plug was drawn into the tubing and injected onto the μNIMS until droplets

Published on 05 December 2016. Downloaded by Concordia University, Montreal on 19/01/2018 16:00:41.

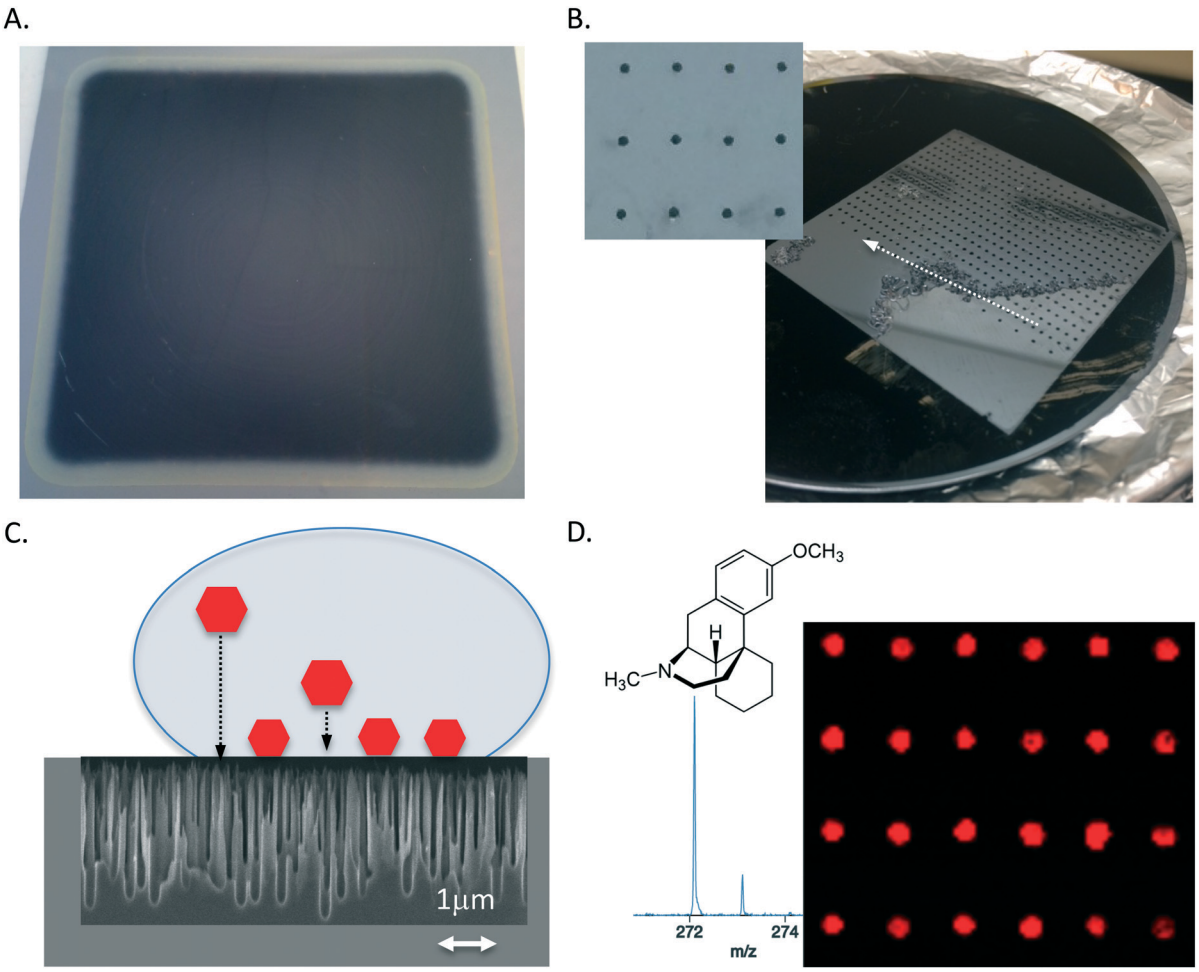

Fig. 2 NIMS chips. A. Photo of a conventional NIMS chip, B. photo of patterned array of 640 μNIMS pads on silicon wafer with PDMS protective gasket partially peeled away, C. analyte sorbs onto NIMS pad from droplet D. structure, spectra and mass spectral image of dextromethorphan (272 *m/z*) adsorbed onto surface of μNIMS pads.

filled the central chamber. Droplets were then loaded onto the NIMS in parallel after halting flow (Fig. 4A.), or continuously in series (Fig. 4B.). Please see supplementary video† for examples of each. Droplets were removed from the pad at different times after reaction start as indicated in Fig. 1E. Mass spectrometry imaging and OpenMSI analysis of the spotted array detects both the probe and three hydrolysis products (Fig. 3) and kinetic analysis at both pH values the cellotetraose, G4, is rapidly degraded into G3, G2 and G1 over the course of 50 minutes (Fig. 4) and it is also found that CelE produces similar product distributions at both pH further indicating that it is robust to process conditions, with reaction profile similar to previous work (Deng, 2015).

Discussion

We have described a device for manipulation of 150 nl droplets with subsequent deposition onto the NIMS surface, achieving a significant reagent reduction *vs.* previous work requiring a 20 μl dead volume. This device has the ability to interface with 31 NIMS pads simultaneously and can be physically re-aligned to the next position on the array (which contains 640 pads total). Using the demonstrated device each NIMS array can be used for rapid kinetic characterization of 20 different enzymes or conditions, however modification of protocol could expand that to 620 individual assays at 1 pad per enzyme. Depending on experimental demands, the number of replicates can be modified, *i.e.* to increase the number reaction conditions investigated or to increase time resolution.

The programmable architecture allows μNIMS to place droplets onto the NIMS surface and remove them at different times for analysis of enzyme kinetics. This ability to deposit sample and subsequently remove the droplets enables the device to take advantage of the fluorous phase interactions between the NIMS surface and derivatized substrates and products. While this work focused on relatively clean enzyme assays, this washing step has proven to be important in other applications, such as analysis of enzyme activities from soils (Reindl, 2010).

This device operates *via* electro wetting on dielectric (EWOD) and isn't thought to use dielectrophoresis (DEP).[38,39]

 This journal is © The Royal Society of Chemistry 2017

Published on 05 December 2016. Downloaded by Concordia University, Montreal on 19/01/2018 16:00:41.

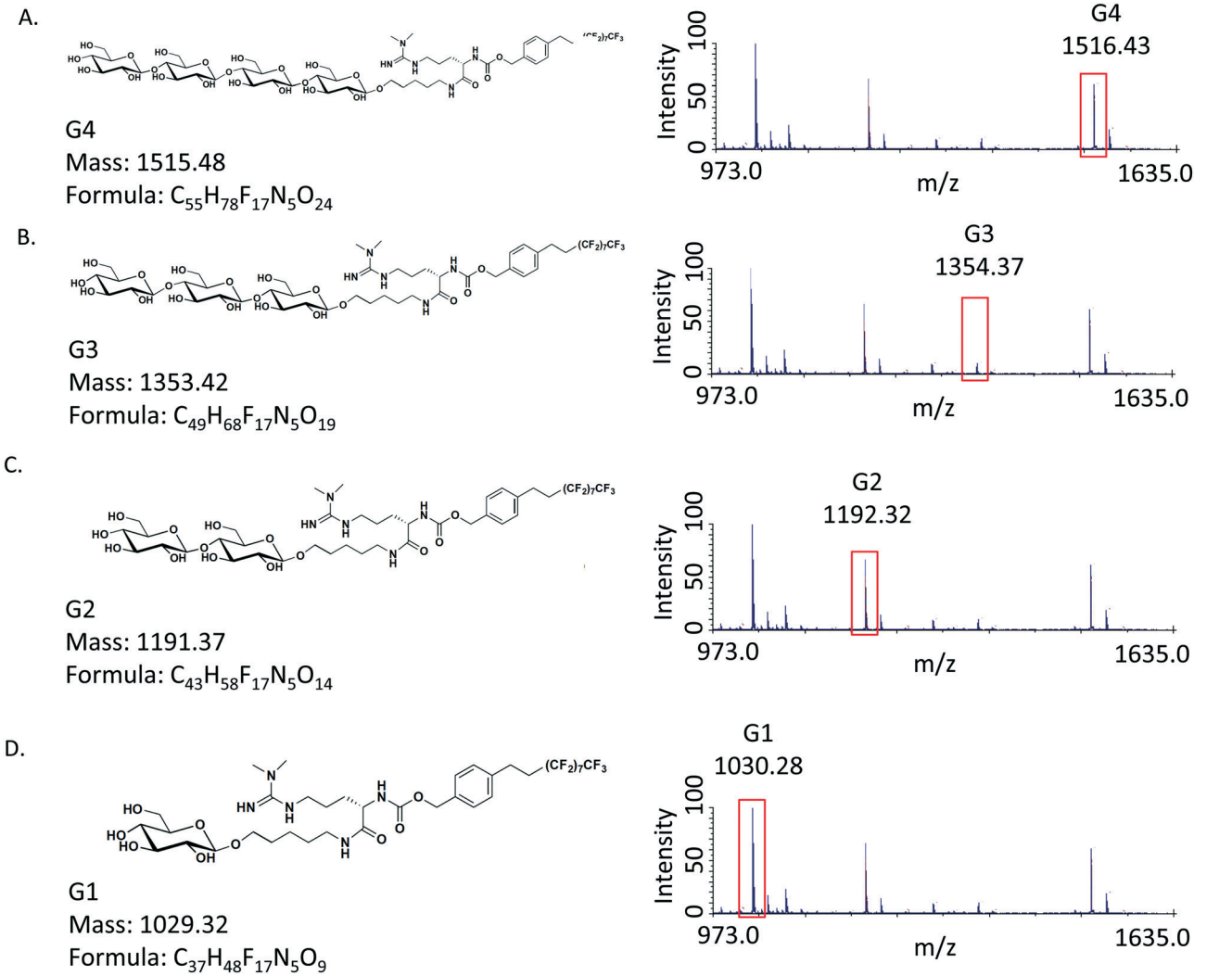

Fig. 3 Probe substrates, products and mass spectra using μNIMS. A. Chemical structure of 1,4-*b*-D-cellotetraose-probe (G4) substrate and mass spectra of G4 substrate 1516 *m/z* (H^+), B. chemical structure of cellotriose-probe (G3) product, mass spectra of G3 product 1354 *m/z* (H^+), C. chemical structure of cellobiose-probe (G2) product, mass spectra of G2 product 1354 *m/z* (H^+), D. chemical structure of glucose-probe (G1) product, and mass spectra of G1 product 1354 *m/z* (H^+).

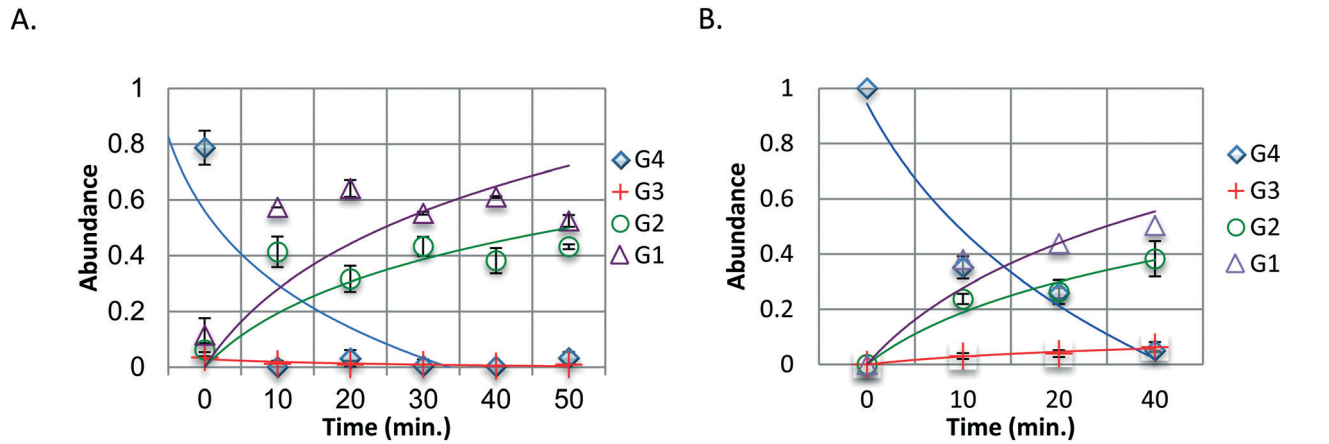

Fig. 4 Enzyme kinetics of CelE-CBM3a as visualized by μNIMS. 1,4-*b*-D-cellotetraose-probe (G4) substrate, to cellotriose-probe (G3) product, cellobiose-probe (G2) and glucose-probe (G1) as visualized using NIMS array from μNIMS, A. time series analysis of CelE in phosphate buffer solution (pH = 6.0) B. time series analysis of CelE in acetate buffer (pH = 5.0), if error bars are not present no deviation was observed.

Published on 05 December 2016. Downloaded by Concordia University, Montreal on 19/01/2018 16:00:41.

This is because aqueous droplets are drawn into and out of the NIMS pocket by their attraction to the charge, which accumulates over the electrodes. The level of droplet control automation was limited to the abilities of the dropbot and microdrop graphical user interface GUI. Impedance detection was used to detect actuation failure, but because of lack of integration with syringe pumps no mitigating contingency could be used. This experiment was monitored and validated visually, which is a limitation. Greater development of dropbot GUI would allow us to take corrective measures when actuation fails. Failure is typically attributed to fabrication imperfection or dust contamination in dielectric layer. In the case of failure of actuation, it is obvious, as the mass spectrometer will not detect the substrate or products.

It is unfortunate that the fluorous oil/aqueous droplet reduces sensitivity. This can possibly be attributed to surfactant interference during ionization, which adheres to the NIMS surface and is not removed by the washing steps negatively impacting NIMS sensitivity. Generally, surfactants are widely known to interfere with biomolecule characterization by mass spectrometry, as a result of their often efficient desorption/ionization, relatively high concentrations, and the fact that they are often heterogenous mixtures resulting in multiple ions.[40] Since surfactants remain key to proper functioning of the chip and it is desirable to develop NIMS compatible surfactants. However, until then, the NIMS surface is functioning as a capture device for the substrates and products for subsequent mass spectrometry imaging.

Device design allowed droplets to be maintained at ±10% standard deviation in size except initially during flow where droplets tended to be larger. This was due to some turbulent mixing which occurred when the fluids came into contact. While droplet reproducibility is desirable, our assay is based on fractional conversion, which we have found to be a very effective approach for controlling experimental variation in NIMS enzyme activity assays.[6] For example, the fractional conversion of G4 into G1 would be [G1]/([G4] + [G3] + [G2] + [G1]). This is essentially an internal normalization that makes these assays less sensitive to variations in droplet volumes and other sources of variations than assays focused on direct measurements of concentration.

Conclusion

In conclusion, we describe first integration of NIMS with microfluidics, and because of common fabrication methods could provide a valuable tool for microfluidic detection in the greater community. We demonstrate our technologies application to a common laborious laboratory task, which can be easily automated. The density of the NIMS grid is scalable and by scaling the currently demonstrated structure to the lower bounds of demonstrated digital microfluidics with the laser resolution of the mass spectrometer. A grid of 50 μm resolution can be used giving the possibility of >100 000 pads per 5 cm^2 NIMS array when scaling the current design. This scale is compatible with the highest scanning resolution of the mass spectrometer (ABsciex MALDI-TOF) and the lowest digital microfluidic demonstration.[41] Electrode density, currently limited to the 120 channels on the dropbot could be overcome by conversion to a lower voltage system, appropriate for lower droplet volumes. Computational control of metabolic experiments stands to vastly increase the scale of experimental data, this is important as the number of variables which act on a biological system simultaneously can affect the phenotype of the organism and be directly related to metabolism, which dynamically changes over time.[7] Our chip setup is similar to a memory array where droplets of enzyme and probe, are actuated to a controlled location on a two dimensional array. While the droplets are only transiently located onto the NIMS pad, the probe sticks, which allows the NIMS array to be removed from the microfluidic system and scanned. Promising further directions for this technology is to develop NIMS 'friendly' surfactants and interface with upstream devices.

Experimental

Reagents

Unless otherwise specified, general use reagents were purchased from Sigma-Aldrich. Microfluidic device fabrication reagents and supplies included SU-8-5, SU-8-2075 and SU-8 Developer from Microchem (Newton, MA), gold and chromium-coated glass slides from Telic (Valencia, CA), indium tin oxide (ITO)-coated glass slides, and silicone wafers from Delta Technologies (Stillwater, MN), Aquapel from TCP Global (San Diego, CA), MF-321 positive photoresist developer from Rohm and Haas (Marlborough, MA), CR-4 chromium etchant from OM Group (Cleveland, OH), and AZ-300 T photoresist stripper from AZ Electronic Materials (Somerville, NJ). Sylgard 184 polydimethylsiloxane (PDMS) was purchased from Dow Corning (Midland, MI). For photopatternable PDMS benzophenone and mixed xylenes were purchased from Sig-ma. For silanization of master molds Trichloro(1*H*,1*H*,2*H*-perfluorooctyl)silane (TPS) was used.

Microfluidic device fabrication

Microfluidic devices were fabricated in house and the University of California Biomolecular Nanotechnology Center (UC Berkeley BNC) Fabrication Center, using a transparent photomask printed at CAD/Art Services Inc. (Bandon, OR). Digital microfluidic electrodes and pads were patterned using photolithography and etching described previously.[26] Briefly chrome Telic wafers pre-coated with AZ1500 positive resist were exposed to UV for 15 s (16 mW cm^2) using an OAI Series 200 aligner (San Jose, CA) and were developed by immersing in MF-321 for ~1 min and rinsed with deionized water (diH_2O). The slide was then hard baked for 1 min at 120 °C using a hotplate. Chrome was etched by immersing the slide with resist in CR-4 for 5 min with gentle agitation. The device was then rinsed with diH_2O and immersed in AZ 300T stripper for 5 min to remove photoresist. The slide was again rinsed with diH_2O. To prepare for dielectric coating,

 This journal is © The Royal Society of Chemistry 2017

Published on 05 December 2016. Downloaded by Concordia University, Montreal on 19/01/2018 16:00:41.

the slide (now with electrodes) was soaked in acetone for 5 min with gentle agitation, rinsed with isopropanol (IPA) and soaked in diH_2O for 5 min with gentle agitation, then dried with N2 gas. Slides were then placed onto a hotplate at 120 °C for 10 min for post baking. The slide was then plasma treated for 5 min using 20% O_2 and RF power of 20 W (Brand) and subsequently coated with 5 μm layer dielectric using SU-8-5 following Microchem protocol. For channel layer a master mold was constructed using SU-8-2075 with a height of 140 μm. Spin speeds, soft and hard bakes, and development times were per Microchem's protocol. After development these were rinsed and dried with IPA and H_2O. These molds were then placed into vacuum desiccator with 200 μl of TPS and let sit overnight for silanization then hard baked for 15 min at 120 °C. To form channels onto electrodes and dielectric layer the master mold was placed into a vacuum desiccator and 5 ml of PDMS (20 : 1 PDMS to curing agent) was poured over the master mold and degassed under vacuum for 1 hour. Prior to molding, electrode/dielectric layer was plasma treated for 5 min using 20% O_2 and RF power of 20 W. To form channels, master mold with PDMS was placed onto hotplate at 100 °C for 1 h with electrode/dielectric layer pressed against the master mold using a 1 kg aluminium block. Master mold was then removed and holes were drilled into the glass electrode layer using a 1/32″ round bottom end mill (Other Machine Co., US) to allow fluidic access. The chip was then sealed against a glass slide and 100 μl of picoglide (Dolomite Microfluidics, UK) was pumped through the channel and let sit for 30 min. This was followed by a rinse with Novec HFE-7500 (3 M, US).

Fabrication of NIMS Array

NIMS arrays were fabricated by coating a silicon wafer with a photopatternable PDMS[34] to selectively etch only small areas of the silicon wafer for subsequent analysis using NIMS. The PDMS mixture was prepared by mixing with the curing agent in a 10 : 1 ratio (m/m). The benzophenone was mixed with the PDMS to a final concentration of 3%, and degassed by centrifugation. The mixture was then spin coated onto a silicon wafer at 2500 rpm for 30 s and exposed to UV (<365 nm) for 10 min under the appropriate photomask. The photomask was position ~100 μm over the substrate for the duration of the exposure. For post exposure bake the substrate was placed in a vacuum oven on top of a piece of cardboard at 120 °C for 2.5 min. Afterward the substrate was developed in toluene for 10s and immediately rinsed with IPA and H_2O. A nitrogen gun with strong flow rate was applied to blow off any particle residues from the substrate's surface. Then it was placed into the etching chamber of a PlasmaLab 100 etching tool (Oxford Instrument) to fabricate nanostructured μNIMS pads by inductively coupled plasma reactive ion etching (ICP-RIE) process. A plasma mixture of SF6 and O_2 at 30/20 gas ratio with 6 mTorr chamber pressure was used here, and the powers of etching chamber and plasma generator chamber were fixed at 5 W and 1000 W, respectively. To balance etching depth and passivation layer formation, a steady cryogenic temperature, −80 °C, was maintained during the etching process. Modified from ref. 16.

Chip assembly and operation

The manifold for holding together the μNIMS system was designed using Blender (Blender.org) and 3D printed using polylactic acid (Ultimaker 2) at 215 °C extrusion temperature (Fig. 1C. i., v.). The overall assembly has five layers (Fig. 1A.), and the microfluidics portion of the assembly consists of four separate layers (Fig. 1B.). The pogo pin contact pads are compressed against the dropbot PCB connector simultaneously the PDMS is compressed against the NIMS chip/ground plate to create a reversible fluidic seal. This allows the NIMS array to be removed from the system and placed in the mass spectrometer once the experiment is completed. The droplet-to-digital microfluidics chip consists of chrome electrodes over a central fluidics channel (Fig. 1). The chip contains two basic functions, a t-junction for droplet generation (Fig. 1A. 1.) and 31 arrayers for droplet actuation over μNIMS pads (Fig. 1A. 2.). The chip layers facilitate droplet actuation where glass substrate, chrome electrodes, dielectric, and fluidics makes the top of the stack for interfacing with the NIMS array, which also functions as a ground plate for droplet actuation (Fig. 1B.). The PDMS fluidic layer seals reversibly to the array, where the central channel (500 μm W × 225 μm H), (Fig. 1A.). The glass layer contains fluidic access ports and is coated with 128 (5 cm L × 500 μm W × 375 μm H) chrome electrodes on the bottom side for directing droplets into pockets (Fig. 1B.). The reversible sealing nature of this technology allows droplets to be deposited onto the array (Fig. 1C.) where the array (Fig. 1C. iv.) is aligned in direct contact with the DMF chip containing the glass, electrodes, dielectric and fluidic layers subsequently allowing removal and placement into the mass spectrometer (MS) for imaging. Briefly, the stack holding the layers are contained within layers 3D printed from polyethylene terephthalate glycol modified (PETG) (Fig. 1C. i. v.), where the bottom layer also contains pogo pins in printed circuit board for integration with dropbot DMF control hardware.[33] An upper gasket made of PDMS sits between the 3D printed chassis and DMF chip to allow reversible sealing of PEEK tubing (Fig. 1C. ii.).

CellE enzyme cocktail was loaded onto the device by prefilling tubing with 5 μl plugs of pre-mixed reaction. Enzyme plugs were broken into droplets at the t-junction (flow rate: 0.05 μl s^{-1} reaction cocktail, 0.2 μl s^{-1} HFE 7500) to fill the central fluidics chamber (Fig. 2A.). The droplets were transported using flow, which competes with the force of digital droplet actuation where unless flow is sufficiently low (or stopped) it will prevent droplet actuation into the micoNIMS wells. Once in position, droplets of enzyme cocktail were actuated onto all of the μNIMS pads where they were incubated for a period of time (Fig. 4B.). At 10 min intervals, 6 droplets are synchronously removed (Fig. 4C.). Protocols have long

Published on 05 December 2016. Downloaded by Concordia University, Montreal on 19/01/2018 16:00:41.

wait sequences, with short bursts of fast actuation (250 ms, 90 V, 10 000 Hz). This fast actuation functions to move droplets from the central chamber, in and out of the pocket containing the NIMS active pad. Allowing substrate and product to sorb onto the NIMS. This is consistent with the normal operation of NIMS (Gao, 2016).

Dextromethorphan analysis

Droplets of dextromethorphan (1 mg ml^{-1} in H_2O) were used for rudimentary testing of microfluidic functions, and for NIMS array evaluation. Briefly 150 nl spots were actuated over NIMS pads to evaluate sorption of small molecules into the NIMS pads. Pads where dextromethorphan droplets were actuated showed clear ionization only on the NIMS pads not on surrounding structures. These results were matrix free, dextromethorphan ionization was sufficient using only NIMS.

Enzymatic assays

Briefly, purified endogluconase, CelE-CBM3a was reacted with 1,4-*b*-D-cellotetraose-probe (G4) substrate-probe G4 in either 50 mM phosphate buffer (pH = 6) or 100 mM acetate buffer (pH = 5) and analysed every 10 min using μNIMS. Reaction solutions were premixed in an 0.5 ml eppendorf tube, by adding 4 μl buffer, 1 μl substrate and 1 μl CelE-CBM3a (CelE) enzyme (240 μg ml^{-1}) and premixing to a final volume of 6 μl. A plug of 5 μl was drawn into tubing using syringe pumps and injected onto the μNIMS where plug was broken into droplets so it filled the central chamber, subsequently droplets were then actuated onto the NIMS pads. Reactions were performed at room temperature and droplets were removed from the pad at different times after reaction start as indicated in Fig. 5.

Mass spectral analysis

Mass spectral analysis was performed on a 5800 MALDI/TOF (ABSciex, US). The instrument was operated in positive ionization mode with a laser intensity of 4150 and focus mass of 1200 *m*/*z*. The NIMS array was imaged with a 50 μm laser step resolution after the chip was coated with universal MALDI matrix (20 mg ml^{-1} MeOH). Data was processed using OpenMSI spot set analysis tools.[36]

Acknowledgements

This work conducted by the Joint BioEnergy Institute was supported by the Office of Science, Office of Biological and Environmental Research, of the U.S. Department of Energy under Contract No. DE-AC02-05CH11231.

References

1 G. A. Khoury, H. Fazelinia, J. W. Chin, R. J. Pantazes, P. C. Cirino and C. D. Maranas, *Protein Sci.*, 2009, **18**, 9–11.
2 B. Kuhlman, G. Dantas, G. C. Ireton, G. Varani, B. L. Stoddard and D. Baker, *Science*, 2003, **5649**, 1364–1368.
3 L. L. Looger, M. A. Dwyer, J. J. Smith and H. W. Hellinga, *Nature*, 2003, **423**, 185–190.
4 H. W. Hellinga, *Proc. Natl. Acad. Sci. U. S. A.*, 1997, **94**, 10015–10017.
5 O. Kucher and F. H. Arnold, *Trends Biotechnol.*, 1997, **15**, 523.
6 K. Deng and T. R. Northen, *Front. Bioeng. Biotechnol.*, 2015, 3(153), DOI: 10.3389/fbioe.2015.00153.
7 J. Heinemann, B. Noon, M. J. Mohigmi, A. Mazurie, D. L. Dickensheets and B. Bothner, *J. Am. Soc. Mass Spectrom.*, 2014, 1755–1762.
8 A. R. Buller, S. Brinkmann-Chen, D. K. Romney, M. Herger, J. Murciano-Calles and F. H. Arnold, *J. Biol. Chem.*, 2015, **112**(47), 14599–14604.
9 K. J. Yong and D. J. Scott, *Biotechnol. Bioeng.*, 2015, **112**(3), 438–446.
10 M. P. Greving, G. J. Patti and G. Siuzdak, *Anal. Chem.*, 2011, **83**(1), 2–7.
11 T. Northen, T. R. Northen, O. Yanes, M. T. Northen, D. Marrinucci and W. Uritboonthai, *Nature*, 2007, **449**, 1033–1036.
12 O. Yanes, H. Woo, T. R. Northen, S. R. Oppenheimer, L. Shriver and J. Apon, *Anal. Chem.*, 2009, **81**(8), 2969–2975.
13 R. A. Heins, X. Cheng, S. Nath, K. Deng, B. P. Bowen and D. C. Chivian, *ACS Chem. Biol.*, 2014, **9**(9), 2082–2091.
14 J. Wu, C. S. Hughes, P. Picard, S. Letarte, M. Gaudreault and D. A. Nicoll-Griffith, Assays, *Anal. Chem.*, 2005, **79**(12), 396–401.
15 X. Cheng, J. Hiras, K. Deng, B. Bowen and B. A. Simmons, *Front. Microbiol.*, 2013, **4**, 1–7.
16 J. Gao, M. De Raad, B. P. Bowen, R. N. Zuckermann and T. R. Northen, *Anal. Chem.*, 2016, **88**(3), 1625–1630.
17 X. Lin, Q. Wang, P. Yin, L. Tang, Y. Tan and H. Li, *Metabolomics*, 2011, **7**(4), 549–558.
18 X. Feng, B. Liu, J. Li and X. Liu, *Lab Chip*, 2015, **2000**, 535–557.
19 D. Gao, *Lab Chip*, 2013, 3309–3322.
20 H. Moon, A. R. Wheeler, R. L. Garrell, J. A. Loo and C. J. Kim, *Lab Chip*, 2006, **6**(9), 1213.
21 I. Barbulovic-Nad, H. Yang, P. S. Park and A. R. Wheeler, *Lab Chip*, 2008, **8**(4), 519–526.
22 J. Evans, *Microfluid. Nanofluid.*, 2009, 75–89.
23 B. Hadwen, G. R. Broder, D. Morganti, A. Jacobs, C. Brown and J. R. Hector, *Lab Chip*, 2012, **100**, 3305–3313.
24 H. Moon, A. R. Wheeler, R. L. Garrell, J. A. Loo and C.-J. C. Kim, *Lab Chip*, 2006, **6**(9), 1213–1219.
25 W. Reindl, K. Deng, J. M. Gladden, G. Cheng, A. Wong and S. W. Singer, *Energy Environ. Sci.*, 2011, **4**(8), 2884.
26 S. C. C. Shih, P. C. Gach, J. Sustarich, B. A. Simmons, P. D. Adams and A. K. Singh, *Lab Chip*, 2015, **15**(Il), 225–236.
27 S. C. C. Shih, G. Goyal, P. W. Kim, N. Koutsoubelis, J. D. Keasling and P. D. Adams, *ACS Synth. Biol.*, 2015, **4**(10), 1151–1164.
28 W. Reindl and T. Northen, *Anal. Chem.*, 2010, **82**(9), 3751–3755.
29 G. J. Patti, H. Woo, O. Yanes, L. Shriver, D. Thomas and W. Uritboonthai, *Anal. Chem.*, 2010, **82**(1), 4271–4278.

 This journal is © The Royal Society of Chemistry 2017

Published on 05 December 2016. Downloaded by Concordia University, Montreal on 19/01/2018 16:00:41.

30 R. R. Pompano, W. Liu, W. Du and R. F. Ismagilov, *Annu. Rev. Anal. Chem.*, 2011, **4**(1), 59–81.
31 P. C. Gach, S. C. C. Shih, J. Sustarich, J. D. Keasling, N. J. Hillson and P. D. Adams, *ACS Synth. Biol.*, 2016, **5**(5), 426–433.
32 T. Thorsen, R. W. Roberts, F. H. Arnold and S. R. Quake, *Phys. Rev. Lett.*, 2001, **86**(18), 4163–4166.
33 R. Fobel, C. Fobel and A. R. Wheeler, *Appl. Phys. Lett.*, 2013, **193513**, 1–5.
34 A. A. S. Bhagat, P. Jothimuthu and I. Papautsky, *Lab Chip*, 2007, **7**, 1192–1197.
35 J. J. Thomas, Z. Shen, J. E. Crowell, M. G. Finn and G. Siuzdak, *Proc. Natl. Acad. Sci. U. S. A.*, 2001, **98**(9), 4932–4937.
36 O. Rubel, A. Greiner, S. Cholia, K. Louie, E. W. Bethel and T. R. Northen, *Anal. Chem.*, 2013, **85**(21), 10354–10361.
37 K. Deng, T. E. Takasuka, R. Heins, X. Cheng and L. F. Bergeman, *ACS Chem. Biol.*, 2014, **9**(7), 1470–1479.
38 M. Vallet, M. Vallade and B. Berge, *Eur. Phys. J. B*, 1999, **11**(4), 583–591.
39 J. Buehrle, S. Herminghaus and F. Mugele, *Phys. Rev. Lett.*, 2003, **91**(8), 86101.
40 L. H. Cohen and A. L. Gusev, *Anal. Bioanal. Chem.*, 2002, **373**(7), 571–586.
41 Y. Lin, E. R. F. Welch and R. B. Fair, *Sens. Actuators, B*, 2012, **173**, 338–345.